



OPEN ACCESS

EDITED BY

Wei He,
China University of Geosciences, China

REVIEWED BY

Song Fanhao,
Chinese Research Academy of
Environmental Sciences, China
Hua Ma,
Chongqing University, China
Changxiao Li,
Southwest University, China

*CORRESPONDENCE

Hongwei Fang,
✉ fanghw@tsinghua.edu.cn

SPECIALTY SECTION

This article was submitted to
Biogeochemical Dynamics,
a section of the journal
Frontiers in Environmental Science

RECEIVED 01 December 2022

ACCEPTED 27 December 2022

PUBLISHED 17 January 2023

CITATION

Wang K, Fang H, He G, Huang L, Cui Z,
Gao Q, Xu S, Wang D, Wu X and He D
(2023), Optical and molecular diversity of
dissolved organic matter in sediments of
the Daning and Shennong tributaries of the
Three Gorges Reservoir.

Front. Environ. Sci. 10:1112407.

doi: 10.3389/fenvs.2022.1112407

COPYRIGHT

© 2023 Wang, Fang, He, Huang, Cui, Gao,
Xu, Wang, Wu and He. This is an open-
access article distributed under the terms
of the [Creative Commons Attribution
License \(CC BY\)](https://creativecommons.org/licenses/by/4.0/). The use, distribution or
reproduction in other forums is permitted,
provided the original author(s) and the
copyright owner(s) are credited and that
the original publication in this journal is
cited, in accordance with accepted
academic practice. No use, distribution or
reproduction is permitted which does not
comply with these terms.

Optical and molecular diversity of dissolved organic matter in sediments of the Daning and Shennong tributaries of the Three Gorges Reservoir

Kai Wang¹, Hongwei Fang^{1*}, Guojian He¹, Lei Huang¹,
Zhenghui Cui², Qifeng Gao¹, Song Xu¹, Dianchang Wang³,
Xinghua Wu³ and Ding He^{4,5}

¹State Key Laboratory of Hydro-Science and Engineering, Department of Hydraulic Engineering, Tsinghua University, Beijing, China, ²China Renewable Energy Engineering Institute, Beijing, China, ³China Three Gorges Corporation, Beijing, China, ⁴Department of Ocean Science and Hong Kong Branch of the Southern Marine Science and Engineering Guangdong Laboratory (Guangzhou), The Hong Kong University of Science and Technology, Hong Kong, China, ⁵State Key Laboratory of Marine Pollution, City University of Hong Kong, Hong Kong, China

Introduction: Damming significantly modifies the function of natural river networks and influences sediment dynamics with a reservoir's operation. The dissolved organic matter (DOM) in reservoir sediments severely affects carbon flow from land to sea. However, the properties of DOM (e.g., quantity and quality) in reservoir sediments and their relationship with carbon cycling remain unclear as complex reservoir construction interrupts the environmental processes.

Methods: This study characterizes the optical and molecular properties of sediment water-extractable organic matter (WEOM) in the Daning and Shennong tributaries of the world's largest reservoir—the Three Gorges Reservoir (TGR)—by applying optical techniques and ultrahigh-resolution Fourier transform ion cyclotron resonance mass spectrometry (FT-ICR MS).

Results and Discussion: We first assessed the link between light-absorbing components and the individual molecules in WEOM, which were significantly different than DOM in water and indicated that there might be an intrinsic variation between DOM in sediment and in water. Then, with the unique optical–molecular property linkage assessed, multiple sources (autochthonous and terrestrial) were identified, and a declining trend of terrestrial and recalcitrant WEOM was revealed from the tributaries upstream to downstream. Finally, through covariance analysis of the properties between WEOM and sediment particles, we demonstrated that the WEOM dynamic was most likely regulated by hydrologic sorting-induced particle size and mineral composition variations of sediment. Moreover, assessment between lability and WEOM molecular properties suggested that the WEOM dynamic likely contributes to carbon burial in the reservoir. This study emphasizes the influence of dam construction on organic matter accumulation and riverine carbon cycling.

KEYWORDS

WEOM, particle properties, FT-ICR MS, carbon burial, Three Gorges Reservoir

1 Introduction

Rivers serve as connectors in the transportation of material from land to sea, and deliver organic carbon (OC) (approximately 0.45 Pg yr^{-1}) to the ocean (Cole et al., 2007; Regnier et al., 2013). The transportation and transformation of dissolved organic matter (DOM) in riverine sediments links to the sequestration of OC and involves in the carbon cycling between continental and oceanic carbon pools (Bao et al., 2019; Han et al., 2021; Ni and Li, 2023). Therefore, the investigation of water-extractable organic matter (WEOM) from sediment, a crucial component of DOM in sediments with characteristics of high activity and mobility and could be involved in various biogeochemical processes, has become an important component of organic matter quality assessment (Bahureksa et al., 2021; Zhang et al., 2021). For instance, environment context variation (e.g., urbanization and soil erosion) has been proved to be recorded in organic matter in sediments (Darrow et al., 2017; Garzon-Garcia et al., 2017; Yang et al., 2021), which would consequently be imprinted in the composition and sources of WEOM (Dzulkafli et al., 2021; Ni et al., 2021). Therefore, clarifying the dynamic of WEOM (e.g., quantity and quality) is critical to understanding the biogeochemical processes and carbon cycling mechanism in the aquatic ecosystem.

Considering the complexity of DOM in the environment (e.g., water or sediment)—a mixture of various compounds (Hedges et al., 1992; Jaffé et al., 2008)—multiple techniques from the bulk to molecular levels have been introduced to DOM analysis (Wang et al., 2019). Optical techniques, including ultraviolet-visible spectroscopy (UV-Vis) for CDOM analysis and excitation-emission matrixes (EEMs) for FDOM analysis, have been widely applied for high-efficiency analysis of the light-absorbing components of DOM (e.g., chromophoric dissolved organic matter—CDOM; fluorescent dissolved organic matter—FDOM) (Coble, 1996; Cawley et al., 2012a; Cawley et al., 2012b). To exhibit the subtle characteristics of DOM, molecular techniques have also been integrated into the characterization of DOM (Kujawinski, 2002; Dittmar et al., 2008). Molecules (e.g., CHO, CHON, and CHOS) with different environmental behaviors can be identified through the high resolution of Fourier transform ion cyclotron resonance mass spectrometry (FT-ICR MS) (McKnight et al., 2001; Schmidt et al., 2009; Melendez-Perez et al., 2016). Moreover, the combination of UV-Vis or EEMs with FT-ICR MS has been applied to characterize DOM in water and gives a relatively more comprehensive insight into DOM behavior (Stubbins et al., 2014; Wagner et al., 2015; He et al., 2020). However, whether the linkage regime of the optical and molecular information of DOM in water is consistent with that in sediment is still unknown, limiting further understanding of the properties of DOM.

The Three Gorges Reservoir (TGR), located on the Yangtze River, with a multi-year regulation function (water storage: 39.3 billion cubic meters; flood control: 22.15 billion cubic meters), is the largest artificial reservoir in the world. The construction and operation of TGR is the typical interference of the riverine ecosystem of the Yangtze River (the third-longest river in the world). The TGR altered the hydrological context (e.g., flow regime, water retention period, and water levels) of the watershed and exerted a significant influence on biogeochemical processes (e.g., primary productivity), especially in tributaries (Yang et al., 2006; Guo et al., 2012; Arif et al., 2022). Various works have been conducted on the dynamic of DOM in water of TGR and demonstrates

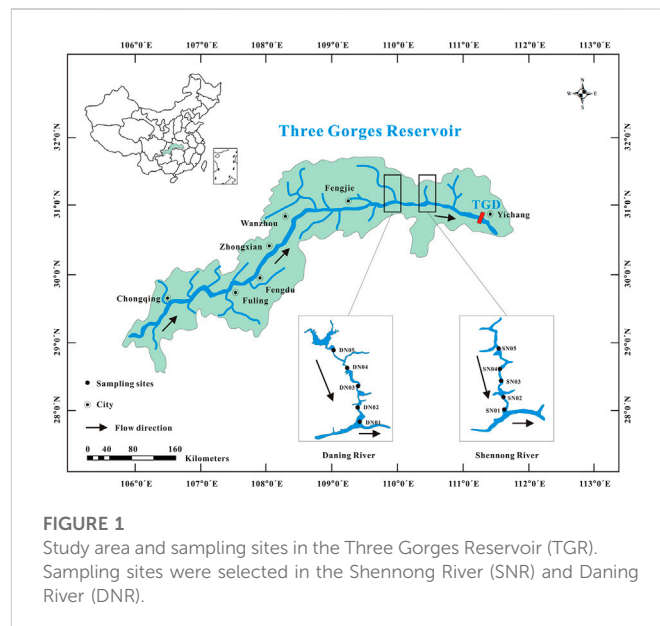


FIGURE 1

Study area and sampling sites in the Three Gorges Reservoir (TGR). Sampling sites were selected in the Shennong River (SNR) and Daning River (DNR).

that reservoir management influences DOM transformation (He et al., 2020; Wang et al., 2021a; Wang et al., 2021b), but systematic investigation on DOM in sediment is still lacking.

In this work, representative tributaries of the TGR—the Shennong River (SNR) and Daning River (DNR)—were chosen to investigate the characteristics of WEOM in sediment. Sediment particle properties and WEOM optical and molecular characteristics were depicted to: a) assess the linkage regime of the optical-molecular properties of DOM in sediment; b) determine the composition and sources of WEOM; c) conduct a preliminary evaluation of the role played by WEOM in the carbon cycling of the TGR. This investigation would provide a subtle insight into organic matter characterization in sediments and devote to dynamic clarification of contaminant relating with organic matter.

2 Methodology

2.1 Sites and sample collection

The TGR was constructed on the lower end of the upper reaches of the Yangtze River. It covers about $5.8 \times 10^4 \text{ km}^2$, straddles the Daba Mountains and southern Sichuan Plateau, and covers the low river gorges as well as the parallel valleys of eastern Sichuan. The TGR has a conventional maximum storage level of 175 m and a minimum storage level of 145 m (Chen et al., 2022; Ding et al., 2022). The SNR and DNR are typical tributaries of the TGR and are, respectively, ca. 75 km and 123 km from the Three Gorges Dam (Figure 1).

Ten sampling sites were set along the SNR and DNR to investigate the variability in WEOM chemistry (Figure 1). Five representative sampling sites were located along the SNR (SN01–SN05) and DNR (DN01–DN05) each, from upstream to downstream (<30 km). The sampling was conducted on 31 May 2018 in a period of water-level decline. We collected ca. 0–2 cm depth sediments as surface sediments. All samples were transported within 48 h to the lab in an icebox for WEOM extraction.

WEOM was extracted according to Hur et al. (2014). Specifically, a 2-mm filter was applied to air-dried sediment samples. Then, a 1 g

sediment sample was mixed with 100 mL water (Mili-Q). The ratio of sediment–water followed Wang et al. (2021c), which was determined by a series of sediment/water ratio gradient extraction experiments. The sediment–water mixture was shaken (200 rpm) by a rotary shaker in the dark. The supernatant was collected and passed through 0.22 μm membrane filters (Millipore Express) to obtain WEOM for further analysis.

2.2 Particle property analysis

The minerals in the sediments were characterized based on X-ray diffraction (XRD) analysis with Cu-K α radiation (40 Kv, 100 mA). The scanning ranges varied from 3° to 70°. The analysis of minerals was carried out on Jade 9 with ICDD. The particle size of sediments was determined by a laser particle size analyzer (Horiba LA-920) after ultrasonic dispersion (Yuan et al., 2020).

The OC content (OC%) in the sediments were measured by a Thermo Scientific FLASH2000 Series CNS Elemental Analyzer (He et al., 2020). Before OC analysis, 2 M HCl was used to treat air-dried sediments (~0.2 g) to remove carbonate. Acid-treated samples were then rinsed with Mili-Q water to pH = 7. Finally, an isotope ratio mass spectrometer (Thermo Scientific) was applied to determine the table carbon isotope ($\delta^{13}\text{C}$) of sedimentary organic matter.

2.3 WEOM analysis

Nutrient concentration including PO_4^{3-} , SiO_3^{2-} , and DIN (e.g., $\text{NO}_3\text{-N}$, $\text{NO}_2\text{-N}$, $\text{NH}_4\text{-N}$) was measured by a segmented flow colorimetric auto-analyzer (Bran + Luebbe). Dissolved organic carbon (DOC) concentration of 0.22 μm filtered WEOM was determined by a TOC analyzer (Shimadzu TOC-L) with University of Miami deep-sea standards. 3D-EEMs and UV-Vis were measured on an Aqualog absorption-fluorescence spectrometer (Horiba) according to Wang et al. (2021a). In 3D-EEMs measurement, a 1 cm path length quartz cuvette was hired. We used Mili-Q water as blank and conducted the scan over 240–650 nm with increments of 3 nm and a scan integration time of 1s. In sample measurement, the blank was subtracted, and the inner filter effects was removed. Several optical parameters applied in various studies were also introduced in this work. We calculated specific ultraviolet absorbance at 254 nm (SUVA_{254}) for the aromaticity degree of CDOM (Weishaar et al., 2003), biological index (BIX) for autotrophic productivity (Huguet et al., 2009), freshness index (FrI) for the proportion of recently produced or fresh DOM (Parlanti et al., 2000), and humification index (HIX) for the humification degree of FDOM (Ohno, 2002). For detailed analysis of EEMs, a DOMFluor toolbox-based PARAFAC model was introduced (Stedmon and Bro, 2008).

WEOM was extracted for molecular analysis by solid-phase extraction (SPE) with PPL cartridges (Agilent Bond Elut). FT-ICR MS was introduced to WEOM analysis to reflect the molecular properties. The analysis was conducted with a Bruker Solarix FT-ICR MS (15.0 T) with an electrospray ionization (ESI) source (Research Center for Eco-Environmental Sciences, Chinese Academy of Sciences) (Tang et al., 2021). Molecular formulae, ranging from 120 to 1,000 Da, were assigned by the specific element limitation ($\text{C}_{\leq 80}$, $\text{H}_{\leq 200}$, $\text{O}_{\leq 40}$, $\text{N}_{\leq 3}$, and $\text{S}_{\leq 2}$) with a

C/N threshold of >4. The element content, ratios, modified aromaticity index (AI_{mod}), and double bond equivalent (DBE) were obtained by weighted average calculation (Wang et al., 2019). Molecule types (e.g., peptides, H/C: 1.5–2.0, N > 0; unsaturated aliphatic compounds: UA, H/C: 1.5–2.0, N = 0; polycyclic aromatics: PCAs, $\text{AI}_{\text{mod}} > 0.66$; polyphenols: polyp, AI_{mod} : 0.50–0.66; highly unsaturated compounds: HU, $\text{AI}_{\text{mod}} < 0.50$, H/C < 1.5) were categorized following previous studies (Martínez-Pérez et al., 2017). The molecular lability index (MLB_L) was also calculated in WEOM molecular analysis (D'Andrilli et al., 2015).

2.4 Statistical analyses

To evaluate the regime of optical–molecular linkage in WEOM, the Spearman's correlation between the molecular peaks of FT-ICR MS and spectral information was assessed (Stubbins et al., 2014). The optical and FT-ICR MS data of DOM in water of TGR was obtained from He et al. (2020), and a comparison of optical–molecular linkage between DOM in sediment and water of TGR was conducted. A principal component analysis (PCA) was introduced for WEOM dynamic clarification.

3 Results

3.1 Particle properties of sediment

Median particle size (MPS) ranged from 4.1–18.7 μm and 5.0–17.6 μm in the SNR and DNR sediment, respectively (Supplementary Figure S1). MPS values declined from tributary upstream to downstream in both SNR and DNR. In terms of mineral composition, various minerals, including quartz, illite, feldspar, calcite, dolomite, and chlorite, were identified. The proportion of quartz, feldspar, and dolomite declined from tributary upstream to downstream in SNR and DNR, while the proportion of illite, calcite, and chlorite varied inversely (Figure 2).

OC% values ranged 0.6%–2.2% and 0.6%–0.8% in SNR and DNR, respectively (Supplementary Figures S2A, C). OC% values declined from tributary upstream to downstream in SNR and DNR (Supplementary Figure S2A, C). $\delta^{13}\text{C}$ values varied from –28.3‰ to –26.1‰ in SNR and –27.3‰ to –26.1‰ in DNR and demonstrated an increasing trend from tributary upstream to downstream (Supplementary Figures S2B, D).

3.2 Bulk and optical property of WEOM

There was no significant spatial variation of nutrient concentration (PO_4^{3-} , SiO_3^{2-} , and DIN) in both SNR (PO_4^{3-} : 1.13–4.54 μM ; SiO_3^{2-} : 9.07–33.30 μM ; DIN: 28.09–93.58 μM) and DNR (PO_4^{3-} : 1.08–2.48 μM ; SiO_3^{2-} : 12.78–20.14 μM ; DIN: 46.72–89.27 μM) (Supplementary Table S1). DOC concentration ranged 197.50–235.83 μM and 174.17–224.17 μM in SNR and DNR, respectively (Supplementary Table S1). To assess the proportion of DOC in sediment, it was isolated in the unit of mg C/g sediment: DOC in SNR and DNR varied 0.24–0.28 mg C/g sediment and 0.21–0.27 mg C/g sediment (Supplementary Table S1),

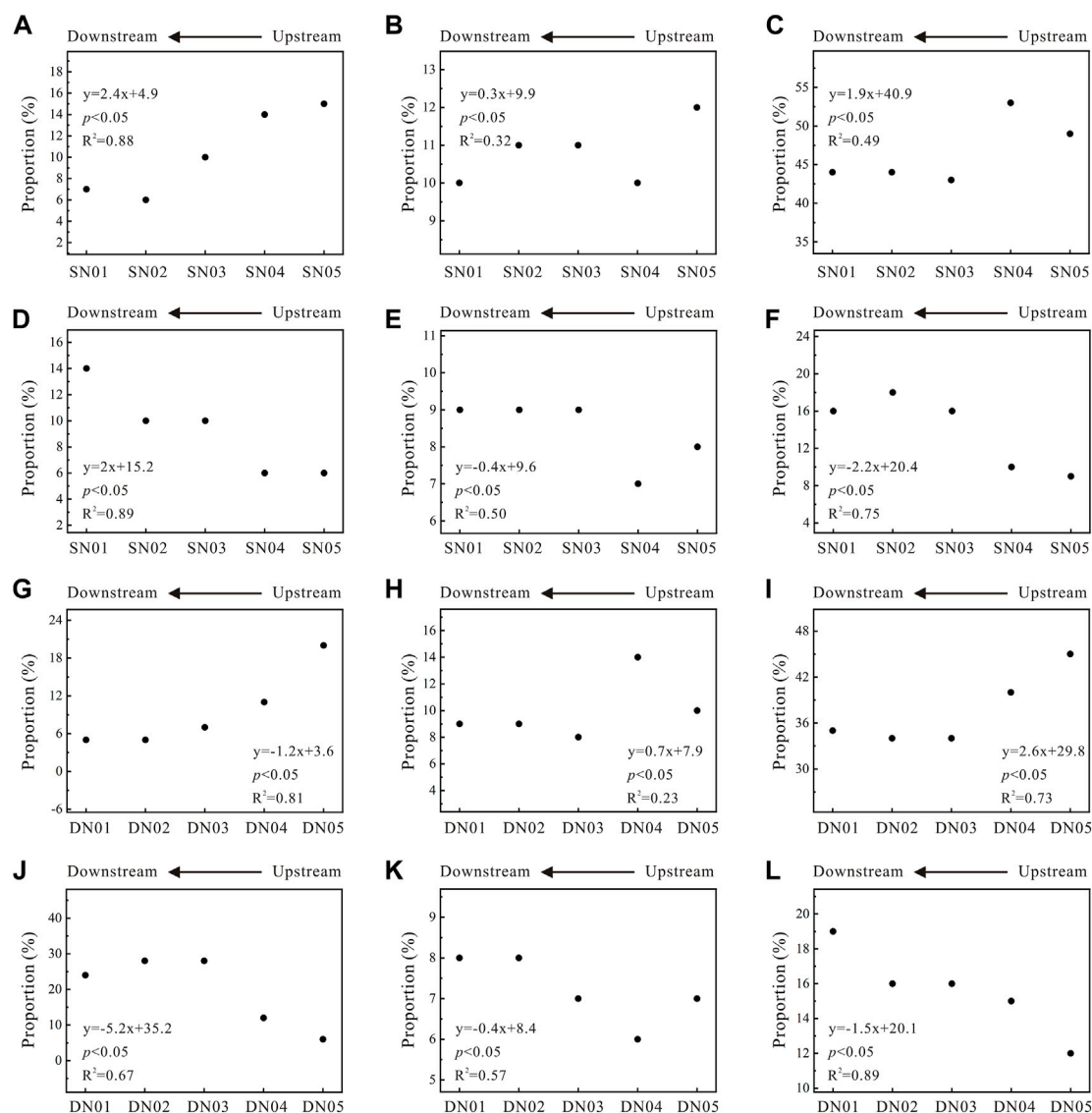


FIGURE 2
Mineral composition of sediments in SNR and DNR: (A) dolomite, (B) feldspar, (C) quartz, (D) calcite, (E) chlorite, and (F) illite in SNR; (G) dolomite, (H) feldspar, (I) quartz, (J) calcite, (K) chlorite, and (L) illite in DNR.

respectively, which were higher than that in surface sediments of the urban river (averaged 0.10 ± 0.02 mg C/g sediment) (Zhang et al., 2021).

SUVA₂₅₄ relating to the aromaticity of CDOM in WEOM, ranged 4.89–5.36 L mg-C⁻¹ m⁻¹ in SNR and 4.17–5.21 L mg-C⁻¹ m⁻¹ in DNR (Supplementary Table S2). HIX, representing the humification of FDOM in WEOM, varied 0.55–0.81 in SNR and 0.47–0.56 in DNR (Supplementary Table S2). Both SUVA₂₅₄ and HIX decreased upstream to downstream in SNR and DNR (Figure 3, Supplementary Figure S3). On the other hand, there was a downstream toward increase in BIX (ranging 0.47–0.52 in SNR and 0.47–0.57 in DNR) and FrI (ranged 0.47–0.52 in SNR and 0.47–0.56 in DNR), which hints the autotrophic productivity in both tributaries (Figure 3). The semi-quantitative EEMs-PARAFAC further supported the variation of light-absorbing components in WEOM. Specifically, four fluorescent components were identified: humic-like components (C1, C2, and C3) and protein-like component

(C4) (Supplementary Figure S4). Compared to downstream, there was a higher relative proportion of C1, C2, and C3 upstream, while the relative proportion of C4 varied inversely (Figure 3).

3.3 Molecular property of WEOM

A total of 9,018 and 10,196 unique compounds were characterized by FT-ICR MS in SNR and DNR, respectively; the number of identified formulae in each sample varied between 5,749 and 6,884: an average of $2,378 \pm 54$ CHO compounds, $2,494 \pm 61$ CHON compounds, $1,396 \pm 91$ CHOS compounds, and 89 ± 10 CHONS compounds in SNR and $2,560 \pm 15$ CHO compounds, $2,585 \pm 95$ CHON compounds, $1,443 \pm 78$ CHOS compounds, and 103 ± 8 CHONS compounds in DNR were identified (Supplementary Table S3). CHO compounds were present in relatively higher abundance than N- and

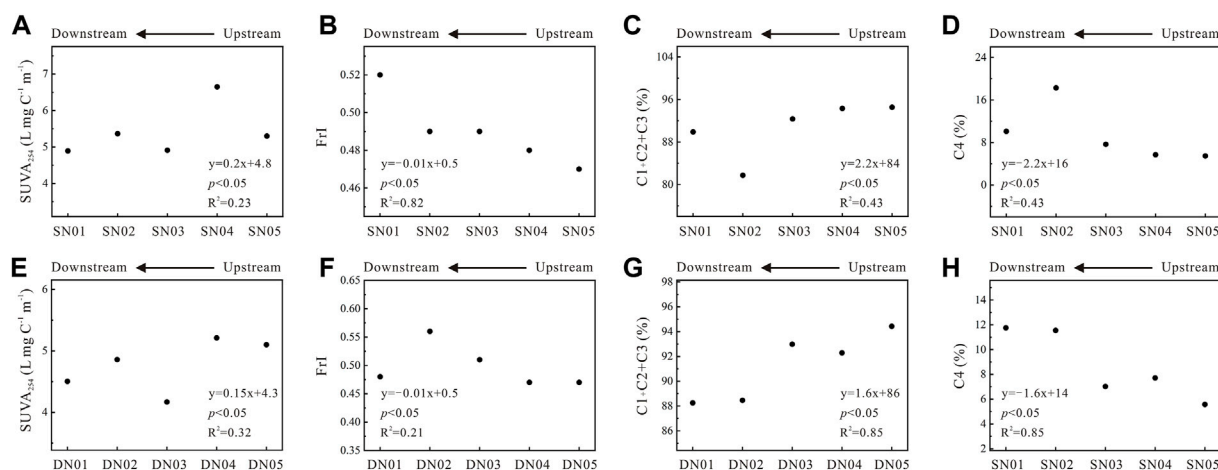


FIGURE 3

Optical properties of water-extractable organic matter (WEOM) in SNR and DNR. (A) SUVA₂₅₄, (B) FrI, (C) C1+C2+C3, and (D) C4 in SNR; (E) SUVA₂₅₄, (F) FrI, (G) C1+C2+C3, and (H) C4 in DNR. Note: SUVA₂₅₄, specific ultraviolet absorbance at 254 nm; FrI, freshness index; C1, Component 1; C2, Component 2; C3, Component 3; C4, Component 4.

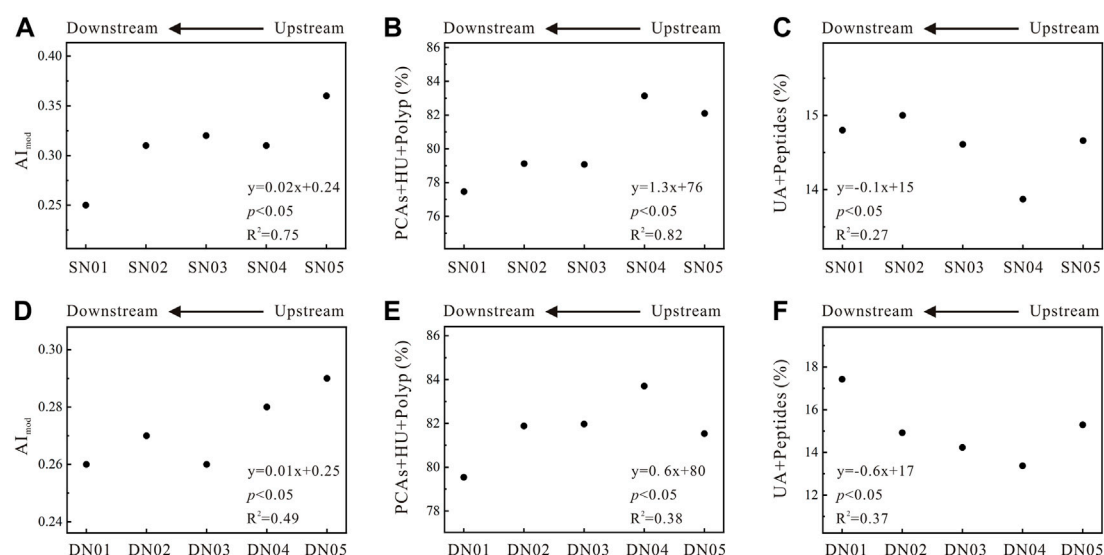


FIGURE 4

Molecular properties of WEOM in SNR and DNR. (A) AI_{mod}, (B) PCAs + HU + polyp, and (C) UA + peptides in SNR; (D) AI_{mod}, (E) PCAs + HU + polyp, and (F) UA + peptides in DNR. Note: AI_{mod}, modified aromaticity index; PCAs, polycyclic aromatics; HU, highly unsaturated compounds; polyp, polyphenols; UA, unsaturated aliphatic compounds.

S-containing compounds. CHO, CHON, CHOS, and CHONS compounds exhibited homogeneity in relative abundance in upstream and downstream samples. AI_{mod}, DBE, and m/z values declined from the tributaries upstream to downstream, whereas MLB_L values increased (Figure 4). In addition, PCAs, polyp, and HU abundance varied 77.5%–83.1% in SNR and 79.5%–83.7% in DNR and declined in the tributaries upstream to downstream (Figure 4). Peptides and aliphatic compounds abundances varied 13.9%–15.0% in SNR and 13.4%–17.4% in DNR and increased from the tributaries upstream to downstream (Figure 4).

4 Discussion

4.1 Optical–molecular linkage regime of DOM in sediment and the difference from that in water

Optical parameters including FrI, BIX, and SUVA₂₅₄ exhibited significant correlations with AI_{mod}, DBE, MLB_L, and m/z ($r > 0.5$ or < -0.5), whereas no significant correlation was observed between HIX with molecular information (Figure 5A), preliminarily indicating that there was a heterogeneity linkage

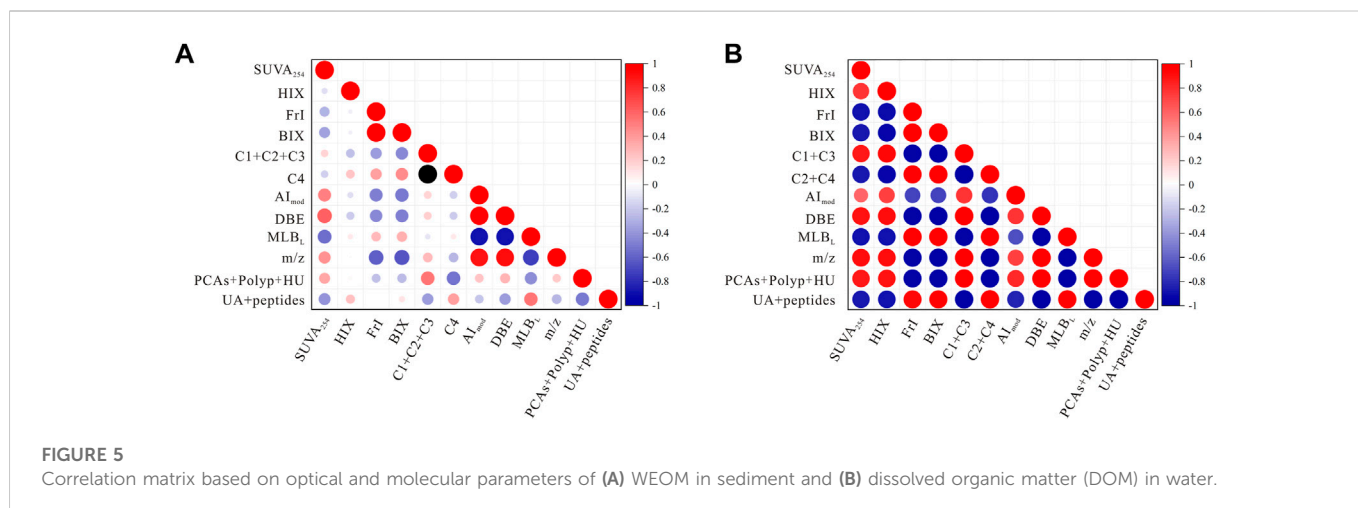


FIGURE 5
Correlation matrix based on optical and molecular parameters of (A) WEOM in sediment and (B) dissolved organic matter (DOM) in water.

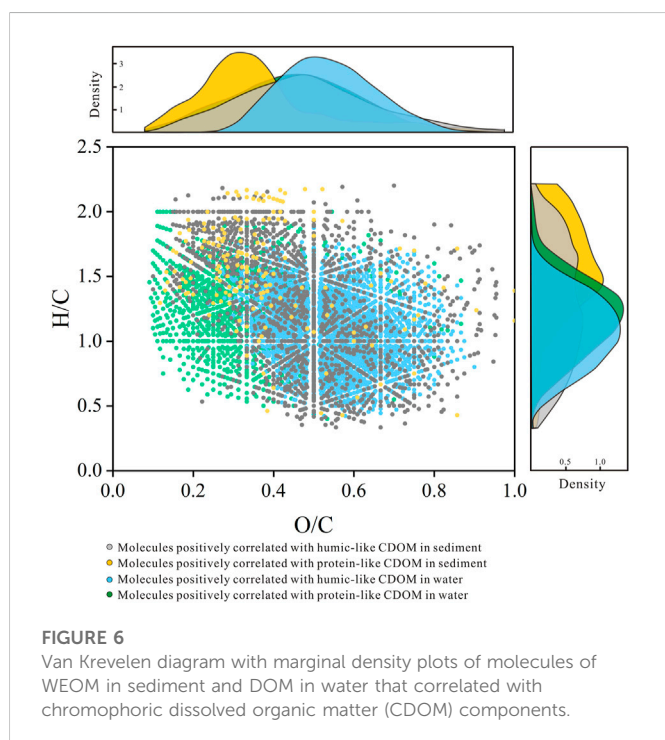
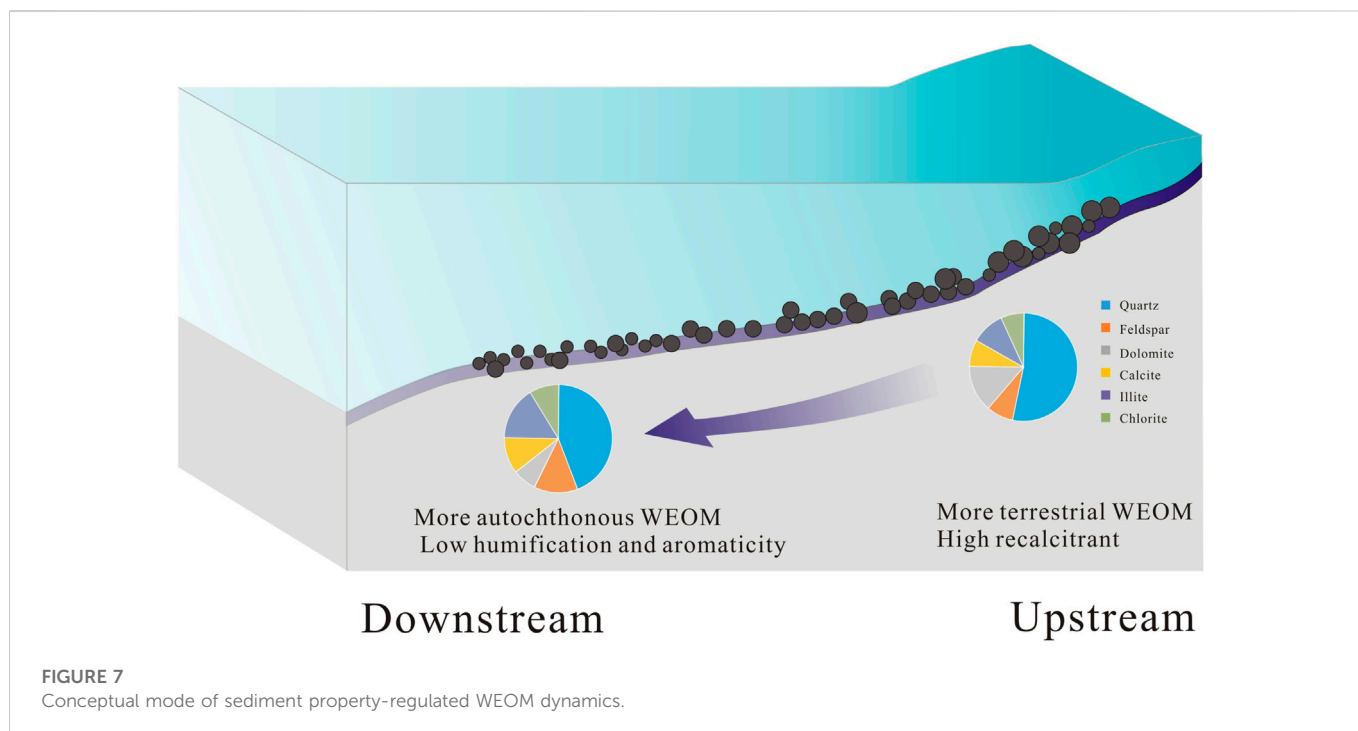


FIGURE 6
Van Krevelen diagram with marginal density plots of molecules of WEOM in sediment and DOM in water that correlated with chromophoric dissolved organic matter (CDOM) components.

between the optical and molecular properties of DOM in sediment. Specifically, the significant positive correlation between $SUVA_{254}$ and AI_{mod} , DBE, and m/z demonstrated that CDOM compounds with high aromaticity tracked closely with high aromatic and unsaturated molecules with high molecular weight (Weishaar et al., 2003; Huguet et al., 2009), which might be derived from terrestrial sources (Seidel et al., 2015; Painter et al., 2018). The negative linkage among FrI, BIX and AI_{mod} , DBE, m/z indicated that the autotrophic activity derived CDOM pool is probably linked to low aromaticity, unsaturated molecules (Wagner et al., 2015) (Figure 5A), which could be involved in microbial activities (Zhou et al., 2019; Messetta et al., 2020). Humic material has been proven to consist of various macromolecules derived from the assemblage of individual, small molecules by the linkage of dispersive forces

(Simpson et al., 2002; Romera-Castillo et al., 2014), which might result in the ambiguous linkage between HIX, the parameter relating to the humification degree of CDOM, and molecular information (Figure 5A). In terms of specific compounds, humic-like and protein-like components correlate significantly to terrestrially sourced PCAs, polyp, HU (Seidel et al., 2015), and autochthonously sourced peptides and aliphatic compounds (Kellerman et al., 2018), respectively, exhibiting the equal effectiveness of CDOM components and molecular groups in tracking DOM sources. Therefore, the covariance of the optical and molecular properties of DOM in sediment could be influenced by biogeochemical processes (e.g., microbial activity) and sources.

In previous studies, the combination of optical characteristics with FT-ICR MS has greatly broadened our understanding of the complex behaviors of DOM in water (Herzprung et al., 2012; Stubbins et al., 2014; Timko et al., 2014; Kellerman et al., 2015; Wagner et al., 2015). To comprehensively assess the characteristics of DOM in sediment, we compared the optical–molecular linkage between DOM in sediment and in water (He et al., 2020) (Figures 5, 6), further demonstrating the unique association of the optical and molecular properties of DOM in sediments (Figures 5, 6). Compared to DOM in water, which exhibited homogeneously significant correlation among all optical and molecular parameters, the optical and molecular property of DOM in sediment presented limited association (Figure 5). Especially, HIX and $SUVA_{254}$, the parameters represent humification degree and aromaticity of CDOM, respectively, and always tracked the similar molecule pools in water DOM (Williams et al., 2010; Dixon et al., 2014; He et al., 2020), showed significant different associated behaviors in sediment DOM. This was also consistent with the observation of Singh et al. (2014), indicating that HIX might be less effective in tracing aromatic compound in sediment DOM than in water DOM for structured matrices of sediment that influence the function of DOM (Zsolnay, 2003), or that there was limited overlap between humified and aromatic molecules of DOM in sediment. Moreover, to provide finer insights into the difference between optical–molecular linkage in sediment and water DOM, an optical component (e.g., humic-like and protein-like components)-related van Krevelen Diagram with marginal density plots is presented (Figure 6). A highly divergent distribution of CDOM associated molecules from DOM in sediment and water was observed,



indicating the intrinsic difference between DOM in sediment and water. Specifically, less molecules correlated with CDOM components of DOM in sediment than that in water were observed, in consistent with the correlation variation of optical and molecular parameters (Figure 5). Molecules positively correlated with humic-like CDOM exhibited relatively higher O/C and lower H/C than those positively correlated with protein-like CDOM in both DOM in sediment and in water, demonstrating that, although sources or cycling behaviors varied, there was still universal molecular information in natural DOM (Zark and Dittmar, 2018).

4.2 Control on composition and property of WEOM

With the bulk, optical, and molecular properties of WEOM characterized, the variation of WEOM in tributaries was revealed. In the SNR and DNR, the proportion of terrestrially derived WEOM (e.g., PCAs, HU, and polyp compounds) decreased significantly along the tributaries upstream to downstream transects, while autochthonous derived WEOM (e.g., UA and peptide) increased ($p < .01$) (Figures 3, 4) (Seidel et al., 2015). Meanwhile, $\delta^{13}\text{C}$, SUVA_{254} , HIX, AI_{mod} , m/z , and DBE exhibited higher values upstream than downstream, indicating that WEOM upstream tends to be more aromaticity with a higher molecular weight and unsaturation degree than that downstream (Figures 3, 4) (Hansen et al., 2016). PCA provided the preliminary insights into the variation dynamic of WEOM, which exhibited that the higher terrestrial signaled upstream samples had positive score values of PC1 and appeared around MPS, quartz, feldspar, and dolomite, while the higher autochthonous signaled downstream or tributary estuary samples had negative score values on PC1 and appeared around calcite, illite, and chlorite (Supplementary Figure S5). The analysis indicated that sediment property (e.g., mineral

composition and particle size) was involved severely in the dynamic of WEOM and hinted that sediment property influenced the dynamics of WEOM.

In particular, the sediment grain size could be sorted by hydrological conditions, resulting in relatively larger grain sizes of sediment particles upstream and smaller downstream. Grain size could influence the structure of the pore system in particles and the relative number of reactive surface groups per unit mass of particle by spatial and diffusional confinement (Vereecken et al., 1989); this might provide relatively more effective binding points for H-enriched compounds (e.g., autochthonously derived OM) in small particles and enhance the carrying of relatively unsaturated compounds (e.g., terrestrially derived OM) with O atoms or OH groups in large particles. This was consistent with the positive relationship between HIX, SUVA_{254} , AI, and MPS and the negative relationship between BIX, FrI, and MPS (Supplementary Figure S6). In terms of mineral composition, a complex dynamic of OM molecules on the mineral-OM interface was revealed, which might be constrained by various factors, including the surface chemistry of minerals and OM property (Leinemann et al., 2018). This multiple-factor influenced and complex combination of minerals and OM would lead to the preferred binding of mineral and OM molecules (Kalbitz et al., 2005). Specifically, the higher abundance of quartz, feldspar, and dolomite upstream might prefer the adsorption of OM molecules with high aromaticity (Kaiser and Guggenberger, 2000; Kalbitz et al., 2000). Moreover, the environment context might influence the interfacial energy of quartz, feldspar, and dolomite, enabling recalcitrant molecules to coexist. This study indicated significant covariance among quartz, feldspar, or dolomite and individual molecules with high molecular weight and aromaticity (Supplementary Figure S6). PCAs, HU, and polyp compounds were enriched with quartz, feldspar, or dolomite content (Supplementary Figure S6). Calcite, illite, and chlorite have a

relatively high specific surface area (SSA) (Cui et al., 2017; Wu et al., 2020), which might favor the accumulation of high saturated organic compounds. In addition to the surface topography, the crystal structures of illite and chlorite (e.g., the sheet of edge-sharing octahedra and corner-sharing tetrahedra) would limit crystal growth and maintain particle size (Chen et al., 2018) and, consequently, might also facilitate H-enriched OM molecule accumulation. This is also consistent with the close covariance between individual molecules with low molecular weight and high H/C (e.g., peptides and unsaturated aliphatics) and calcite, illite, and chlorite in this study (Supplementary Figure S6). Based on this, a sediment property-dependent conceptual model of WEOM dynamics was developed (Figure 7). In this model, tributary sediment regulates the dynamic of WEOM, which leads to higher terrestrial WEOM accumulation upstream and higher autochthonous WEOM accumulation downstream by regulating the distribution of a mineral matrix and sediment particle size (Figure 7).

4.3 Implications for carbon burial

Reservoirs are hot spots of carbon cycling with autochthonous and allochthonous carbon mixing, and they accommodate various carbon-related biogeochemical processes (Dean and Gorham, 1998; Battin et al., 2009; Tranvik et al., 2009; Li et al., 2019). With the quality assessment of WEOM, an essential form of organic carbon buried, the carbon dynamic information in reservoir would be hinted. Bio-incubation experiments of OM in the TGR (He et al., 2020) have demonstrated the positive relationship between the aromaticity of OM molecules and bio-degradation resistance (Wang et al., 2021c) (Supplementary Figure S7). This indicates that high terrestrially aromatic WEOM in the tributary upstream would be at the high end of bio-degradation resistance. Furthermore, the high autochthonous WEOM, which was less aromatic and more labile, accelerated the downstream tributary, which has a much greater water depth (>50 m) with lower oxygen content and water temperature than those upstream (Huang et al., 2019). The low oxygen content and water temperature would limit heterotrophic microbial activity and might constrain the biodegradation of autochthonous WEOM downstream (Bond-Lamberty and Thomson, 2010; Davidson et al., 2012). Thus, reservoir operation inducing WEOM dynamics is likely to be beneficial to OM preservation both upstream and downstream and devotes to carbon burial in tributaries. However, assessing the quantitative contribution of WEOM in tributaries to carbon burial in the whole reservoir requires further research.

This study has some limitations. For instance, considering the limited efficiency of water extraction, only some minerals (e.g., calcite, illite, and chlorite) which could fix OM molecules by adsorption were analyzed; the analysis of other minerals (e.g., iron-bearing minerals) which also fix OM molecules in a complex mode needed to be integrated into a more efficient extraction (e.g., base extraction) to delineate the dynamic of OM in more detail. Nevertheless, a novel insight into carbon sequestration and burial in the TGR was presented in this investigation, contributing to better clarification of carbon cycling interference by reservoir construction and operation, especially in the global context of the increasing construction of reservoirs.

5 Conclusion

This work investigated the water-extractable organic matter (WEOM) dynamic in two typical tributaries—the Shennong River (SNR) and Daning River (DNR) of the Three Gorges Reservoir (TGR). The bulk, optical, and molecular properties of WEOM were characterized by a comprehensive analysis of stable carbon isotopes ($\delta^{13}\text{C}$), ultraviolet-visible spectroscopy (UV-Vis), excitation–emission matrixes (EEMs), and Fourier transform ion cyclotron resonance mass spectrometry (FT-ICR MS). With the optical–molecular linkage of WEOM revealed, a relatively higher proportion of terrestrially derived WEOM with a higher aromaticity degree but a lower proportion of autochthonously derived WEOM upstream rather than downstream was characterized. The association assessment between sediment property and WEOM molecules indicated that particle size and mineral variation might regulate WEOM dynamics in tributaries. Combining with lability analysis of OM molecules, we concluded that WEOM dynamic in tributary induced by reservoir construction might devote to carbon burial. Considering the reservoir blooming globally, further quantitatively research on WEOM dynamics in reservoirs would be needed to better assess the anthropogenic interference on riverine carbon cycling.

Data availability statement

The original contributions presented in the study are included in the article/Supplementary Material; further inquiries can be directed to the corresponding author.

Author contributions

KW: investigation, formal analysis, writing—original draft, and writing—review and editing. HF: conceptualization, writing—original draft, and writing—review and editing. GH: data analysis and writing—review and editing. LH: data analysis and writing—review and editing. ZC: data analysis and writing—review and editing. QG: data analysis and writing—review and editing. SX: data analysis and writing—review and editing. DW: writing—review and editing. XW: writing—review and editing. DH: data analysis and writing—review and editing.

Funding

This study was supported by Postdoctoral Science Foundation of China (2021M701931), National Key Research and Development Program of China (2022YFC3201802), National Natural Science Foundation of China (U2040214 and 12272209), the Hong Kong Branch of Southern Marine Science and Engineering Guangdong Laboratory (Guangzhou) (SMSEGL20SC01), and funding support from the Center for Ocean Research in Hong Kong and Macau (CORE; QNLM20SC01-J).

Conflict of interest

DW and XW were employed by China Three Gorges Corporation.

The remaining authors declare that the research was conducted in the absence of any commercial or financial relationships that could be construed as a potential conflict of interest.

Publisher's note

All claims expressed in this article are solely those of the authors and do not necessarily represent those of their affiliated organizations, or those of the publisher, the editors, and the

reviewers. Any product that may be evaluated in this article, or claim that may be made by its manufacturer, is not guaranteed or endorsed by the publisher.

Supplementary material

The Supplementary Material for this article can be found online at: <https://www.frontiersin.org/articles/10.3389/fenvs.2022.1112407/full#supplementary-material>

References

- Arif, M., Behzad, H. M., Tahir, M., and Li, C. (2022). The impact of ecotourism on ecosystem functioning along main rivers and tributaries: Implications for management and policy changes. *J. Environ. Manag.* 320, 115849. doi:10.1016/j.jenvman.2022.115849
- Bahureksa, W., Tfaily, M. M., Boiteau, R. M., Young, R. B., Logan, M. N., McKenna, A. M., et al. (2021). Soil organic matter characterization by fourier transform ion cyclotron resonance mass spectrometry (FT ICR MS): A critical review of sample preparation, analysis, and data interpretation. *Environ. Sci. Technol.* 55 (14), 9637–9656.
- Bao, R., Blattmann, T. M., McIntyre, C., Zhao, M., and Eglinton, T. I. (2019). Relationships between grain size and organic carbon 14C heterogeneity in continental margin sediments. *Earth Planet. Sci. Lett.* 505, 76–85. doi:10.1016/j.epsl.2018.10.013
- Battin, T. J., Luysaert, S., Kaplan, L. A., Aufdenkampe, A. K., Richter, A., and Tranvik, L. J. (2009). The boundless carbon cycle. *Nat. Geosci.* 2 (9), 598–600. doi:10.1038/ngeo618
- Bond-Lamberty, B., and Thomson, A. M. (2010). Temperature-associated increases in the global soil respiration record. *Nature* 464 (7288), 579–582. doi:10.1038/nature08930
- Cawley, K. M., Butler, K. D., Aiken, G. R., Larsen, L. G., Huntington, T. G., and McKnight, D. M. (2012a). Identifying fluorescent pulp mill effluent in the Gulf of Maine and its watershed. *Mar. Pollut. Bull.* 64 (8), 1678–1687. doi:10.1016/j.marpolbul.2012.05.040
- Cawley, K. M., Ding, Y., Fourqurean, J., and Jaffé, R. (2012b). Characterising the sources and fate of dissolved organic matter in shark bay, Australia: A preliminary study using optical properties and stable carbon isotopes. *Mar. Freshw. Res.* 63 (11), 1098–1107. doi:10.1071/mf12028
- Chen, J., Zhu, E., Liu, J., Zhang, S., Lin, Z., Duan, X., et al. (2018). Building two-dimensional materials one row at a time: Avoiding the nucleation barrier. *Science* 362 (6419), 1135–1139. doi:10.1126/science.aau4146
- Chen, Z., Song, H., Arif, M., and Li, C. (2022). Effects of hydrological regime on Taxodium ascendens plant decomposition and nutrient dynamics in the Three Gorges Reservoir riparian zone. *Front. Environ. Sci.* 1679. doi:10.3389/fenvs.2022.990485
- Coble, P. G. (1996). Characterization of marine and terrestrial DOM in seawater using excitation-emission matrix spectroscopy. *Mar. Chem.* 51 (4), 325–346. doi:10.1016/0304-4203(95)00062-3
- Cole, J. J., Prairie, Y. T., Caraco, N. F., McDowell, W. H., Tranvik, L. J., Striegl, R. G., et al. (2007). Plumbing the global carbon cycle: Integrating inland waters into the terrestrial carbon budget. *Ecosystems* 10 (1), 172–185. doi:10.1007/s10021-006-9013-8
- Cui, Z., Fang, H., Huang, L., Ni, K., and Reible, D. (2017). Effect of surface heterogeneity on phospor adsorption onto mineral particles: Experiments and modeling. *J. Soils Sediments*.
- D'Andrilli, J., Cooper, W. T., Foreman, C. M., and Marshall, A. G. (2015). An ultrahigh-resolution mass spectrometry index to estimate natural organic matter lability. *Rapid Commun. Mass Spectrom.* 29 (24), 2385–2401. doi:10.1002/rcm.7400
- Darrow, E. S., Carmichael, R. H., Calci, K. R., and Burkhardt, W. (2017). Land-use related changes to sedimentary organic matter in tidal creeks of the northern Gulf of Mexico. *Limnol. Oceanogr.* 62 (2), 686–705. doi:10.1002/lno.10453
- Davidson, E. A., Samanta, S., Caramori, S. S., and Savage, K. (2012). The Dual Arrhenius and Michaelis-Menten kinetics model for decomposition of soil organic matter at hourly to seasonal time scales. *Glob. Change Biol.* 18 (1), 371–384. doi:10.1111/j.1365-2486.2011.02546.x
- Dean, W. E., and Gorham, E. (1998). Magnitude and significance of carbon burial in lakes, reservoirs, and peatlands. *Geology* 26, 535–538.
- Ding, D., Arif, M., Liu, M., Li, J., Hu, X., Geng, Q., et al. (2022). Plant-soil interactions and C:N:P stoichiometric homeostasis of plant organs in riparian plantation. *Front. Plant Sci.* 13, 979023. doi:10.3389/fpls.2022.979023
- Dittmar, T., Koch, B., Hertkorn, N., and Kattner, G. (2008). A simple and efficient method for the solid-phase extraction of dissolved organic matter (SPE-DOM) from seawater. *Limnol. Oceanogr. Methods* 6 (6), 230–235. doi:10.4319/lom.2008.6.230
- Dixon, J. L., Osburn, C. L., Paerl, H. W., and Peierls, B. L. (2014). Seasonal changes in estuarine dissolved organic matter due to variable flushing time and wind-driven mixing events. *Estuar. Coast. Shelf Sci.* 151, 210–220. doi:10.1016/j.ecss.2014.10.013
- Dzulkaflī, N. F., Mahdzir, A., and Hara, H. (2021). Bulk chemical and optical spectroscopy characterisations of dissolved organic matter extracted from the tropical coastal sediment. *J. Mar. Sci. Eng.* 9 (9), 997. doi:10.3390/jmse9090997
- Garzon-Garcia, A., Lacey, J. P., Olley, J. M., and Bunn, S. E. (2017). Differentiating the sources of fine sediment, organic matter and nitrogen in a subtropical Australian catchment. *Sci. total Environ.* 575, 1384–1394. doi:10.1016/j.scitotenv.2016.09.219
- Guo, H., Hu, Q., Zhang, Q., and Feng, S. (2012). Effects of the three gorges dam on Yangtze River flow and river interaction with poyang lake, China: 2003–2008. *J. Hydrology* 511, 19–27. doi:10.1016/j.jhydrol.2011.11.027
- Han, L., Wang, Y., Xu, Y., Wang, Y., Zheng, Y., and Wu, J. (2021). Water-and base-extractable organic matter in sediments from lower Yangtze River-Estuary-East China Sea Continuum: Insight into accumulation of organic carbon in the river-dominated margin. *Front. Mar. Sci.* 31. doi:10.3389/fmars.2021.617241
- Hansen, A. M., Kraus, T. E., Pellerin, B. A., Fleck, J. A., Downing, B. D., and Bergamaschi, B. A. (2016). Optical properties of dissolved organic matter (DOM): Effects of biological and photolytic degradation. *Limnol. Oceanogr.* 61 (3), 1015–1032. doi:10.1002/lno.10270
- He, D., Wang, K., Pang, Y., He, C., Li, P., Li, Y., et al. (2020). Hydrological management constraints on the chemistry of dissolved organic matter in the Three Gorges Reservoir. *Water Res.* 187, 116413. doi:10.1016/j.watres.2020.116413
- Hedges, J. I., Hatcher, P. G., Ertel, J. R., and Meyers-Schulte, K. J. (1992). A comparison of dissolved humic substances from seawater with Amazon River counterparts by 13C-NMR spectrometry. *Geochimica Cosmochimica Acta* 56 (4), 1753–1757. doi:10.1016/0016-7037(92)90241-a
- Herzsprung, P., von Tumpling, W., Hertkorn, N., Harir, M., Buttner, O., Bravidor, J., et al. (2012). Variations of DOM quality in inflows of a drinking water reservoir: Linking of van Krevelen diagrams with EEMF spectra by rank correlation. *Environ. Sci. Technol.* 46 (10), 5511–5518. doi:10.1021/es300345c
- Huang, W., Ji, D., Song, L., Liu, D., Huang, Y., Xu, H., et al. (2019). Characteristics and effects of different density flows in tributaries of Three Gorges reservoir in summer. *J. Hydroelectr. Eng.* 38 (4), 63–74.
- Huguet, A., Vacher, L., Relexans, S., Saubusse, S., Froidefond, J. M., and Parlanti, E. (2009). Properties of fluorescent dissolved organic matter in the Gironde Estuary. *Org. Geochem.* 40 (6), 706–719. doi:10.1016/j.orggeochem.2009.03.002
- Hur, J., Lee, B., and Shin, K. (2014). Spectroscopic characterization of dissolved organic matter isolates from sediments and the association with phenanthrene binding affinity. *Chemosphere* 111, 450–457. doi:10.1016/j.chemosphere.2014.04.018
- Jaffé, R., McKnight, D., Maie, N., Cory, R., McDowell, W. H., and Campbell, J. L. (2008). Spatial and temporal variations in DOM composition in ecosystems: The importance of long-term monitoring of optical properties. *J. Geophys. Res. Biogeosciences* 113 (G4). doi:10.1029/2008jg000683
- Kaiser, K., and Guggenberger, G. (2000). The role of DOM sorption to mineral surfaces in the preservation of organic matter in soils. *Org. Geochem.* 31 (7–8), 711–725. doi:10.1016/s0146-6380(00)00046-2
- Kalbitz, K., Schwesig, D., Rethemeyer, J., and Matzner, E. (2005). Stabilization of dissolved organic matter by sorption to the mineral soil. *Soil Biol. Biochem.* 37 (7), 1319–1331. doi:10.1016/j.soilbio.2004.11.028
- Kalbitz, K., Solinger, S., Park, J. H., Michalzik, B., and Matzner, E. (2000). Controls on the dynamics of dissolved organic matter in soils: A review. *Soil Sci.* 165 (4), 277–304. doi:10.1097/00010694-200004000-00001
- Kellerman, A. M., Guillemette, F., Podgorski, D. C., Aiken, G. R., Butler, K. D., and Spencer, R. G. (2018). Unifying concepts linking dissolved organic matter composition to persistence in aquatic ecosystems. *Environ. Sci. Technol.* 52 (5), 2538–2548. doi:10.1021/acs.est.7b05513
- Kellerman, A. M., Kothawala, D. N., Dittmar, T., and Tranvik, L. J. (2015). Persistence of dissolved organic matter in lakes related to its molecular characteristics. *Nat. Geosci.* 8 (6), 454–457. doi:10.1038/ngeo2440

- Kujawinski, E. B. (2002). Electrospray ionization fourier transform ion cyclotron resonance mass spectrometry (ESI FT-ICR MS): Characterization of complex environmental mixtures. *Environ. Forensics* 3 (3-4), 207–216. doi:10.1006/enfo.2002.0109
- Leinemann, T., Preusser, S., Mikutta, R., Kalbitz, K., Cerli, C., Höschel, C., et al. (2018). Multiple exchange processes on mineral surfaces control the transport of dissolved organic matter through soil profiles. *Soil Biol. Biochem.* 118, 79–90. doi:10.1016/j.soilbio.2017.12.006
- Li, S., Mao, R., Ma, Y., and Sarma, V. V. (2019). Gas transfer velocities of CO₂ in subtropical monsoonal climate streams and small rivers. *Biogeosciences* 16 (3), 681–693. doi:10.5194/bg-16-681-2019
- Martínez-Pérez, A. M., Nieto-Cid, M., Osterholz, H., Catalá, T. S., Reche, I., Dittmar, T., et al. (2017). Linking optical and molecular signatures of dissolved organic matter in the Mediterranean Sea. *Sci. Rep.* 7 (1), 3436–3511. doi:10.1038/s41598-017-03735-4
- McKnight, D. M., Boyer, E. W., Westerhoff, P. K., Doran, P. T., Kulbe, T., and Andersen, D. T. (2001). Spectrofluorometric characterization of dissolved organic matter for indication of precursor organic material and aromaticity. *Limnol. Oceanogr.* 46 (1), 38–48. doi:10.4319/lo.2001.46.1.0038
- Melendez-Perez, J. J., Martínez-Mejía, M. J., Awan, A. T., Fadini, P. S., Mozeto, A. A., and Eberlin, M. N. (2016). Characterization and comparison of riverine, lacustrine, marine and estuarine dissolved organic matter by ultra-high resolution and accuracy Fourier transform mass spectrometry. *Org. Geochem.* 101, 99–107. doi:10.1016/j.orggeochem.2016.08.005
- Messetta, M. L., Butturini, A., and Feijoó, C. (2020). Release of dissolved organic matter (DOM) in an autotrophic and productive stream in Pampean region. *Hydrobiologia* 847, 2279–2293. doi:10.1007/s10750-020-04253-7
- Ni, M., and Li, S. (2023). Ultraviolet humic-like component contributes to riverine dissolved organic matter biodegradation. *J. Environ. Sci.* 124, 165–175. doi:10.1016/j.jes.2021.10.011
- Ni, X., Xiao, M., Luo, J., Zhang, H., Zheng, L., Wang, G., et al. (2021). Molecular insights into water-extractable organic phosphorus from lake sediment and its environmental implications. *Chem. Eng. J.* 416, 129004. doi:10.1016/j.cej.2021.129004
- Ohno, T. (2002). Fluorescence inner-filtering correction for determining the humification index of dissolved organic matter. *Environ. Sci. Technol.* 36 (4), 742–746. doi:10.1021/es0155276
- Painter, S. C., Lapworth, D. J., Woodward, E. M. S., Kroeger, S., Evans, C. D., Mayor, D. J., et al. (2018). Terrestrial dissolved organic matter distribution in the North Sea. *Sci. Total Environ.* 630, 630–647. doi:10.1016/j.scitotenv.2018.02.237
- Parlanti, E., Wörz, K., Geoffroy, L., and Lamotte, M. (2000). Dissolved organic matter fluorescence spectroscopy as a tool to estimate biological activity in a coastal zone submitted to anthropogenic inputs. *Org. Geochem.* 31 (12), 1765–1781. doi:10.1016/s0146-6380(00)00124-8
- Regnier, P., Friedlingstein, P., Ciais, P., Mackenzie, F. T., Gruber, N., Janssens, I. A., et al. (2013). Anthropogenic perturbation of the carbon fluxes from land to ocean. *Nat. Geosci.* 6 (8), 597–607. doi:10.1038/ngeo1830
- Romera-Castillo, C., Chen, M., Yamashita, Y., and Jaffé, R. (2014). Fluorescence characteristics of size-fractionated dissolved organic matter: Implications for a molecular assembly based structure? *Water Res.* 55, 40–51. doi:10.1016/j.watres.2014.02.017
- Schmidt, F., Elvert, M., Koch, B. P., Witt, M., and Hinrichs, K. U. (2009). Molecular characterization of dissolved organic matter in pore water of continental shelf sediments. *Geochimica Cosmochimica Acta* 73 (11), 3337–3358. doi:10.1016/j.gca.2009.03.008
- Seidel, M., Yager, P. L., Ward, N. D., Carpenter, E. J., Gomes, H. R., Krusche, A. V., et al. (2015). Molecular-level changes of dissolved organic matter along the Amazon River-to-ocean continuum. *Mar. Chem.* 177, 218–231. doi:10.1016/j.marchem.2015.06.019
- Simpson, A. J., Kingery, W. L., Hayes, M. H., Spraul, M., Humpfer, E., Dvortsak, P., et al. (2002). Molecular structures and associations of humic substances in the terrestrial environment. *Sci. Nat.* 89 (2), 84–88. doi:10.1007/s00114-001-0293-8
- Singh, S., Dutta, S., and Inamdar, S. (2014). Land application of poultry manure and its influence on spectrofluorometric characteristics of dissolved organic matter. *Agric. Ecosyst. Environ.* 193, 25–36. doi:10.1016/j.agee.2014.04.019
- Stedmon, C. A., and Bro, R. (2008). Characterizing dissolved organic matter fluorescence with parallel factor analysis: A tutorial. *Limnol. Oceanogr. Methods* 6 (11), 572–579. doi:10.4319/lom.2008.6.572b
- Stubbins, A., Lapiere, J. F., Berggren, M., Prairie, Y. T., Dittmar, T., and del Giorgio, P. A. (2014). What's in an EEM? Molecular signatures associated with dissolved organic fluorescence in boreal Canada. *Environ. Sci. Technol.* 48 (18), 10598–10606. doi:10.1021/es502086e
- Tang, G., Li, B., Zhang, B., Wang, C., Zeng, G., Zheng, X., et al. (2021). Dynamics of dissolved organic matter and dissolved organic nitrogen during anaerobic/anoxic/oxic treatment processes. *Bioresour. Technol.* 331, 125026. doi:10.1016/j.biortech.2021.125026
- Timko, S. A., Romera-Castillo, C., Jaffé, R., and Cooper, W. J. (2014). Photo-reactivity of natural dissolved organic matter from fresh to marine waters in the Florida Everglades, USA. *Environ. Sci. Process. Impacts* 16 (4), 866–878. doi:10.1039/c3em00591g
- Tranvik, L. J., Downing, J. A., Cotner, J. B., Loiselle, S. A., Striegl, R. G., Ballatore, T. J., et al. (2009). Lakes and reservoirs as regulators of carbon cycling and climate. *J. Oceanol. Limnol.* 54 (6, part 2), 2298–2314.
- Vereecken, H., Maes, J., Feyen, J., and Darius, P. (1989). Estimating the soil moisture retention characteristic from texture, bulk density, and carbon content. *Soil Sci.* 148 (6), 389–403. doi:10.1097/00010694-198912000-00001
- Wagner, S., Jaffé, R., Cawley, K., Dittmar, T., and Stubbins, A. (2015). Associations between the molecular and optical properties of dissolved organic matter in the Florida Everglades, a model coastal wetland system. *Front. Chem.* 3, 66. doi:10.3389/fchem.2015.00066
- Wang, K., Li, P., He, C., Shi, Q., and He, D. (2021a). Density currents affect the vertical evolution of dissolved organic matter chemistry in a large tributary of the Three Gorges Reservoir during the water-level rising period. *Water Res.* 204, 117609. doi:10.1016/j.watres.2021.117609
- Wang, K., Pang, Y., Gao, C., Chen, L., Jiang, X., Li, P., et al. (2021b). Hydrological management affected dissolved organic matter chemistry and organic carbon burial in the Three Gorges Reservoir. *Water Res.* 199, 117195. doi:10.1016/j.watres.2021.117195
- Wang, K., Pang, Y., He, C., Li, P., Xiao, S., Sun, Y., et al. (2019). Optical and molecular signatures of dissolved organic matter in Xiangxi Bay and mainstream of Three Gorges Reservoir, China: Spatial variations and environmental implications. *Sci. Total Environ.* 657, 1274–1284. doi:10.1016/j.scitotenv.2018.12.117
- Wang, K., Pang, Y., Li, Y., He, C., Shi, Q., Wang, Y., et al. (2021c). Characterizing dissolved organic matter across a riparian soil-water interface: Preliminary insights from a molecular level perspective. *ACS Earth Space Chem.* 5 (5), 1102–1113. doi:10.1021/acsearthspacechem.1c00029
- Weishaar, J. L., Aiken, G. R., Bergamaschi, B. A., Fram, M. S., Fujii, R., and Mopper, K. (2003). Evaluation of specific ultraviolet absorbance as an indicator of the chemical composition and reactivity of dissolved organic carbon. *Environ. Sci. Technol.* 37 (20), 4702–4708. doi:10.1021/es030360x
- Williams, C. J., Yamashita, Y., Wilson, H. F., Jaffé, R., and Xenopoulos, M. A. (2010). Unraveling the role of land use and microbial activity in shaping dissolved organic matter characteristics in stream ecosystems. *Limnol. Oceanogr.* 55 (3), 1159–1171. doi:10.4319/lo.2010.55.3.1159
- Wu, Y., Fang, H., Huang, L., and Cui, Z. (2020). Particulate organic carbon dynamics with sediment transport in the upper Yangtze River. *Water Res.* 184, 116193. doi:10.1016/j.watres.2020.116193
- Yang, B., Ljung, K., Nielsen, A. B., Fahlgren, E., and Hammarlund, D. (2021). Impacts of long-term land use on terrestrial organic matter input to lakes based on lignin phenols in sediment records from a Swedish forest lake. *Sci. Total Environ.* 774, 145517. doi:10.1016/j.scitotenv.2021.145517
- Yang, Z., Wang, H., Saito, Y., Milliman, J. D., Xu, K., Qiao, S., et al. (2006). Dam impacts on the changjiang (Yangtze) river sediment discharge to the sea: The past 55 years and after the three gorges dam. *Water Resour. Res.* 42 (4), 1–10. doi:10.1029/2005wr003970
- Yuan, P., Wang, H., Wu, X., and Bi, N. (2020). Grain-size distribution of surface sediments in the bohai sea and the northern yellow sea: Sediment supply and hydrodynamics. *J. Ocean Univ. China* 19 (3), 589–600. doi:10.1007/s11802-020-4221-y
- Zark, M., and Dittmar, T. (2018). Universal molecular structures in natural dissolved organic matter. *Nat. Commun.* 9 (1), 3178–8. doi:10.1038/s41467-018-05665-9
- Zhang, P., Cao, C., Wang, Y. H., Yu, K., Liu, C., He, C., et al. (2021). Chemodiversity of water-extractable organic matter in sediment columns of a polluted urban river in South China. *Sci. Total Environ.* 777, 146127. doi:10.1016/j.scitotenv.2021.146127
- Zhou, L., Zhou, Y., Hu, Y., Cai, J., Liu, X., Bai, C., et al. (2019). Microbial production and consumption of dissolved organic matter in glacial ecosystems on the Tibetan Plateau. *Water Res.* 160, 18–28. doi:10.1016/j.watres.2019.05.048
- Zsolnay, Á. (2003). Dissolved organic matter: Artefacts, definitions, and functions. *Geoderma* 113 (3-4), 187–209. doi:10.1016/s0166-7061(02)00361-0